Polymer Chemistry

ROYAL SOCIETY OF CHEMISTRY

PAPER

View Article Online
View Journal | View Issue

Cite this: *Polym. Chem.*, 2025, **16**, 52

Effects of crosslink density and plasticizer on thermorheological properties of dissociative guanidine-based covalent adaptable networks†

Adelle L. Koenig,[a] Kelsey M. Allis,[b] John S. Lehr[b] and Michael B. Larsen *[a]

We report the effects of varying crosslink density and plasticizer loading on the thermorheological properties of guanidine-based covalent adaptable networks (CANs). CANs engage in dynamic bond-exchange reactions above T_g, resulting in shifts between thermoset-like materials and states capable of flow that can be greatly impacted by network characteristics beyond the exchange reaction itself. The synthesis of guanidine-based CANs by combination of carbodiimide-containing oligomers and various ratios of amine-containing crosslinker molecules and phthalate plasticizer was used to create a library of CANs with varying crosslink density and equal concentrations of guanidine functionalities. Additionally, T_g was tuned by modifying plasticizer loading. CANs at three degrees of crosslink density and three degrees of plasticizer loading were characterized by rheometry and dynamic mechanical analysis. The resulting data indicated that absolute relaxation times varied directly with crosslink density but were largely unaffected by plasticizer content or temperature relative to T_g; thus, plasticizer served to decouple T_g from relaxation dynamics. Moreover, little difference in activation energies was observed between each system, contrasting studies of associative CANs.

Received 7th October 2024,
Accepted 20th November 2024

DOI: 10.1039/d4py01124d

rsc.li/polymers

Introduction

Covalent adaptable networks (CANs) are a broad class of crosslinked polymers based on the application of dynamic covalent chemistry (DCC). These materials incorporate reversible covalent bonds that undergo dynamic bond-exchange reactions under specific circumstances.[1,2] Intrinsic DCC in CANs results in thermoset-like rigidity when reversible bonds are dormant and thermoplastic-like viscoelastic flow upon substantial activation of the dynamic reaction.[3] The effective bridge between thermosets and thermoplastics realized in CANs results in properties such as reprocessability, self-healing, and shape-memory, alongside numerous potential applications.[4–6] Two broad categories based on the bond-exchange mechanism encompass the majority of CANs: associative CANs, also known as vitrimers, possess constant crosslink density (ν_e) throughout the duration of the bimolecular exchange reaction and concomitant relaxation or flow,[7,8] while dissociative CANs exhibit changing ν_e upon activation of the dynamic reaction.[9,10] Experimentally, the line between these categories can blur substantially, as dissociative CANs can display little variation in K_{eq} of the associated and dissociated crosslink states with temperature. As a result, determining the relationship of ν_e to bond-exchange dynamics and the resulting rheological properties can be challenging. Among the currently known dissociative DCCs that display this behavior in CANs are triazolium and anilinium transalkylation,[10,11] oxime transcarbamoylation,[12] and others,[13] while CANs based on Diels–Alder chemistry,[5,14] disulfide exchange,[15–17] thiol-Michael reactions,[18] and hindered urea chemistry show measurable changes in crosslink K_{eq} in the studied temperature windows.[19–21]

In addition to the DCC responsible for crosslink exchange, it has been increasingly recognized that the structural and chemical characteristics of the surrounding polymer matrix have significant effects on CAN properties such as characteristic relaxation time (τ^*) and flow activation energy (E_a). Prepolymer molar mass,[22,23] branching at the point of crosslinking,[24] the concentration of reactive species,[25] crosslinker molar mass,[26,27] polarity,[28] and ν_e have all been found to exert influence over CAN dynamics. In particular, ν_e has emerged as an important governor of CAN behavior. Targeted approaches to study its effects include the manipulation of DCC-reactive species concentration in tandem with crosslink concentration[29–31] and, conversely, decou-

[a]*Department of Chemistry, Western Washington University, Bellingham, WA, 98225, USA. E-mail: mike.larsen@wwu.edu*
[b]*Department of Engineering and Design, Western Washington University, Bellingham, WA, 98225, USA*

†Electronic supplementary information (ESI) available: Additional characterization of oligomers and CANs; data from DMA, stress relaxation, and SAOS analyses; discussion of the sticky Rouse model for unentangled CANs. See DOI: https://doi.org/10.1039/d4py01124d

pling the two by the incorporation of capping agents or similar strategies.[32–34] Additionally, variation in ν_e due to synthetic modifications such as partial permanent crosslinking,[35,36] heterogeneous crosslinking of block prepolymers,[37] and independently activated bond-exchange reactions[38] has been explored.

As dynamic systems, CANs possess intertwining structural, mechanical, and chemical constituents that present challenges in examining specific effects of the polymer matrix. As a result, studies designed to examine particular characteristics like ν_e have varying degrees of control of other related properties, which complicates the attribution of a definitive impact to a specific factor. For example, ν_e has largely been found to relate directly to T_g in both vitrimers and dissociative CANs, as in traditional thermosets.[11,21,26,31,32,34] The relationship of ν_e to rheological properties presents a less cohesive image and may be impacted by the inherent differences in T_g and exchangeable functional group concentration among related systems. For example, ν_e in both vitrimers and dissociative CANs has been found to relate either directly or inversely to τ^*,[23,26,31,32,34,39,40] and dependence of E_a on ν_e can vary substantially.[11,23,27,31,34] Thus, the significant effects of the polymer matrix on CAN systems, as well as its potential for synthetic tunability, make it a suitable pathway for altering CAN dynamics without necessitating modification of the bond-exchange reaction itself. However, much of the work performed thus far in this area examines vitrimers, and the effects of non-DCC components on thermorheological properties of dissociative CANs remain understudied. In particular, the effects of decoupling ν_e from functional group concentration have only been explored in a single system.[32] Furthermore, few studies have directly examined the role of added plasticizers on CAN dynamics,[41] despite their common use to tune thermorheological properties of conventional polymeric materials. We describe herein the synthesis of a library of dissociative guanidine-based CANs varying in ν_e and plasticizer loading while maintaining a constant guanidine concentration (Fig. 1). Chemical, thermal, and rheological properties including T_g, τ^*, E_a, and ν_e were measured by dynamic mechanical analysis (DMA), stress relaxation, and small amplitude oscillatory shear (SAOS) frequency sweeps. We show that ν_e is directly related to τ^* while E_a is relatively constant across network compositions. Further, our results indicate that plasticizer can be used to tune T_g while minimally impacting CAN rheology.

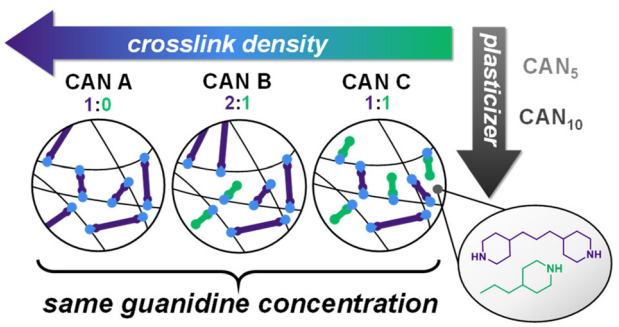

Fig. 1 Synthetic framework of CANs with varying ν_e and plasticizer loading. Difunctional amine crosslinker and monofunctional amine capping agent are shown in purple and green respectively; molar ratios of amine functionalities are given as difunctional : monofunctional species. Plasticizer mass loading (w/w) is given as a subscript, where CAN_0 = 0% w/w plasticizer, CAN_5 = 5% w/w plasticizer, and CAN_{10} = 10% w/w plasticizer.

Experimental section

Materials

Unless otherwise noted, all chemicals were purchased from commercial sources and used as received. Dry tetrahydrofuran (THF) was obtained from an Inert PureSolv solvent purification system.

Instrumentation

^{1}H nuclear magnetic resonance (NMR) spectroscopy was performed on a Bruker Avance III 500 MHz FT-NMR spectrometer. Chemical shifts are reported in delta (δ) units, expressed in parts per million (ppm) downfield from tetramethylsilane using the residual protio-solvent as an internal standard ($CDCl_3$, 7.26 ppm). Infrared (IR) spectroscopy was performed on a Thermo iS10 FT-IR with single-bounce diamond ATR. Thermogravimetric analysis (TGA) was performed on a TA Instruments Q500 with a platinum pan. Temperature ramp experiments were heated at a rate of 10 °C min^{-1} from room temperature to 500 °C under nitrogen flow (40 mL min^{-1}). Dynamic mechanical analysis (DMA) temperature ramp experiments were performed on a TA Instruments Q800 in tension mode. Rectangular samples (approximately 21 mm × 5 mm × 1 mm) were deformed by a 0.025% sinusoidal tensile strain at a frequency of 1 Hz while heating from ambient temperature to 190 °C at a rate of 3 °C min^{-1}. T_g was taken as the peak of tan δ. Rheometry was performed on a TA Instruments DHR-2 Discovery Hybrid Rheometer with 25 mm parallel plate geometry. For strain sweep experiments, samples were held at 170 °C for 300 s, then deformed at 0.001%–5.0% strain at 20 points per decade logarithmically at a constant frequency of 1.0 Hz and a constant axial force of 5 N. For stress relaxation experiments, samples were held at temperature for 60 s, then deformed at 1.0% strain for 1200 s with a constant axial force of 5 N throughout a selected temperature range in 5 °C increments. Continuous relaxation spectra were calculated in TRIOS from the raw stress relaxation data at a given temperature. In spectra with multiple peaks in the continuous relaxation spectrum, the principal peak was determined as that with the largest integration value. For frequency sweep experiments, samples were held at temperature for 60 s, then deformed at an oscillation strain of 1.0% at frequencies of 0.001 Hz–100.0 Hz at 5 points per decade logarithmically with a constant axial force of 5 N throughout a selected temperature range in 5 °C increments. Relaxation times were calculated from the

modulus crossover point ($G' = G''$) as $\tau^*_{cross} = 1/\omega_{cross}$. For frequency sweep experiments, horizontal shift factors (a_T) were determined by manually shifting $\tan\delta$ *versus* ω curves while vertical shift factors (b_T) were determined by manually shifting G^* *versus* ω curves. For stress relaxation experiments, a_T was determined by manually shifting relaxation curves and b_T was obtained by shifting curves such that $G(t)$ at 1 s was equal.

Synthesis and sample processing

Preparation of multifunctional carbodiimide oligomer. In an oven-dried flask under N_2, methylenediphenyl 4,4′-diisocyanate (6.00 g, 24.0 mmol, 1.0 equiv.) and 3-methyl-1-phenyl-2-phospholene 1-oxide (0.230 g, 1.20 mmol, 0.05 equiv.) were dissolved in dry THF (16 mL). To this solution, *p*-tolyl isocyanate (6.95 mL, 55.1 mmol, 2.3 equiv.) was added and the reaction was heated with stirring at 50 °C for 5.5 h with a vent needle. After cooling to room temperature, the solution was precipitated into 10× the reaction volume of chilled 5 : 1 hexanes : methanol using a separatory funnel. The precipitate was recovered by vacuum filtration and dried under reduced pressure at 40 °C overnight to yield oligomer as a white solid (4.53 g, 46.2%) with an average degree of polymerization of 2.5 ± 0.40 by endgroup analysis. Prolonged reaction times led to persistently insoluble material, potentially due to side reactions that result in crosslinking.[42] ^{1}H NMR (500 MHz, $CDCl_3$) δ 7.12–7.04 (m, 29H), 3.93 (s, 5H), 2.33 (s, 6H). ATR-IR: N═C═N 2117 cm^{-1}.

General procedure for synthesis of CAN. Multifunctional carbodiimide oligomer (2.00 g, 2.69 mmol, n + 1 equiv. carbodiimide functionality) was dissolved in THF (28 mL) in a beaker with stirring. In a separate beaker, 1,3-di-4-piperidylpropane, 4-propylpiperidine (amount and equiv. as detailed below) and dioctyl phthalate (5% w/w or 10% w/w if used) were dissolved in THF (14 mL) with stirring. Sonication was used as necessary to aid dissolution. The oligomer solution was chilled in an ice bath for approximately 10 min, after which the stir bar was removed and the amine solution was combined with the oligomer solution by Pasteur pipette. The resulting solution was stirred manually with a metal spatula with THF added as necessary to facilitate stirring. The precipitate and THF were poured into a glass dish and left for solvent evaporation to occur under ambient conditions. The solid was transferred to a vial and dried under reduced pressure at 80 °C overnight. The dried product was crushed into a powder using a mortar and pestle and further dried at 100 °C for 2 h in a vacuum oven to yield CAN as a light yellow powder (3.09 g, 94.6%). ATR-IR: C═N 1575 cm^{-1}. The gel fraction was obtained by soaking a pre-weighed sample of CAN in THF for 24 h, then replacing the THF and soaking another 24 h followed by drying in a vacuum oven at 90 °C for 24 h.

Determination of crosslinker and capping agent stoichiometries. Amounts of 1,3-di-4-piperidylpropane (difunctional crosslinker, D) and 4-propylpiperidine (monofunctional capping agent, M) used in CAN synthesis were determined using eqn (1) and (2):

$$\text{equiv. D} = \left(\frac{x_D}{x_D + x_M}\left(\frac{n+1}{1\ \text{mol CDI oligomer}}\ \frac{1\ \text{mol amine}}{1\ \text{mol CDI}} \times \frac{1\ \text{mol D}}{2\ \text{mol amine}}\right)\right) + 0.005 \quad (1)$$

$$\text{equiv. M} = \left(\frac{x_M}{x_D + x_M}\left(\frac{n+1}{1\ \text{mol CDI oligomer}}\ \frac{1\ \text{mol amine}}{1\ \text{mol CDI}} \times \frac{1\ \text{mol M}}{2\ \text{mol amine}}\right)\right) + 0.005 \quad (2)$$

where x_D and x_M denote molar fractions of D and M, respectively. A slight excess of both crosslinker and capping agent was used to facilitate full conversion of CDI to guanidine.

Procedure for preparation of CAN A_0. Eqn (1) was used to determine equivalence of crosslinker at $x_D = 1$ and $x_M = 0$. Eqn (2) was set to zero. No dioctyl phthalate was used.

Procedure for preparation of CAN A_5. Eqn (1) was used to determine equivalence of crosslinker at $x_D = 1$ and $x_M = 0$. Eqn (2) was set to zero. 5% w/w dioctyl phthalate was used.

Procedure for preparation of CAN B_5. Eqn (1) and (2) were used to determine equivalents of crosslinker and capping agent respectively at $x_D = 2$ and $x_M = 1.5\%$ w/w dioctyl phthalate was used.

Procedure for preparation of CAN C_5. Eqn (1) and (2) were used to determine equivalents of crosslinker and capping agent respectively at $x_D = 1$ and $x_M = 1.5\%$ w/w dioctyl phthalate was used.

Procedure for preparation of CAN A_{10}. Eqn (1) was used to determine equivalence of crosslinker at $x_D = 1$ and $x_M = 0$. Eqn (2) was set to zero. 10% w/w dioctyl phthalate was used.

Procedure for preparation of CAN B_{10}. Eqn (1) and (2) were used to determine equivalents of crosslinker and capping agent respectively at $x_D = 2$ and $x_M = 1.10\%$ w/w dioctyl phthalate was used.

Procedure for preparation of CAN C_{10}. Eqn (1) and (2) were used to determine equivalents of crosslinker and capping agent respectively at $x_D = 1$ and $x_M = 1.10\%$ w/w dioctyl phthalate was used.

Procedure for CAN sample preparation. For samples used in DMA, approximately 220 mg of finely ground CAN was placed into a rectangular 5 mm × 30 mm dry pressing die set (custom-made by MSE Supplies). The die was placed in a benchtop Carver press with heated platens at approximately 169 °C for 30 min with no pressure, then pressed at 2000 psi for 30 min while maintaining heat. Upon removal from the Carver press, the die was cooled to room temperature under ambient conditions before sample retrieval. For samples used in rheometry, approximately 700 mg of finely ground CAN was placed into a circular 25 mm dry pressing die set (MSE Supplies PR0104). The die was placed in a benchtop Carver press with heated platens at approximately 160 °C for 30 min with no pressure, then pressed at 5000 psi for 30 min while maintaining heat. Upon removal from the Carver press, the die

was cooled to room temperature under ambient conditions before sample retrieval.

Results & discussion

Previous work in our group focused on the synthesis and rheological characterization of guanidine-based CANs.[40,43] Upon sufficient heating, *N*,*N*′,*N*″-trisubstituted guanidines undergo a dissociative, reversible exchange of *N*-substituents termed thermal guanidine metathesis (TGM).[44] To prepare CANs, precursors containing multiple carbodiimide (CDI) functionalities can be combined with alkyl diamine crosslinkers to yield guanidine-crosslinked networks. A library of seven guanidine-based CANs was devised to vary ν_e and plasticizer loading while maintaining consistency across other aspects of the polymer matrix. Multifunctional CDI oligomers were synthesized by combining monofunctional aryl isocyanates and diisocyanates in the presence of a phospholene oxide catalyst (Scheme 1).[43] The resulting oligomers were found to have an average degree of polymerization of 2.51 ± 0.40 by ^{1}H NMR endgroup analysis (Fig. S1†). CANs were synthesized by nucleophilic addition of different ratios of difunctional amine crosslinkers and monofunctional amine capping agents together with specific loadings of dioctyl phthalate plasticizer. CANs A, B, and C were prepared in descending order of ν_e: CAN A was synthesized with full crosslinking (difunctional amine only), CAN B was synthesized at a 2 : 1 molar ratio of crosslinker to capping agent, and CAN C was synthesized at a 1 : 1 molar ratio of crosslinker to capping agent based on amine functionalities. Using this synthetic framework, ν_e was changed while maintaining total guanidine concentration. Plasticizer loading was varied in three degrees, with CAN_0, CAN_5, and CAN_{10} variants possessing 0%, 5%, and 10% w/w dioctyl phthalate, respectively. Previous studies on guanidine-based CANs have shown that the addition of phthalates – a common class of plasticizers used in industry – results in lower T_g with no evidence of potential deleterious effects such as side reactions at high temperatures or microphase separation.[40] Accordingly, the chosen plasticizer loadings resulted in an approximately 50 °C range of T_g values for the CAN variants under study (see below). In all cases, ATR FT-IR spectroscopy indicated full conversion of CDI to guanidine, as evidenced by the disappearance of the prominent N=C=N stretching frequency at 2117 cm^{-1} and appearance of a C=N stretching frequency at 1575 cm^{-1} (Fig. S2–S9†). Network formation was further confirmed by sol–gel analysis (Table S1†), with gel fractions generally decreasing with higher monofunctional amine and/or plasticizer loading across CAN formulations. Thermal analysis

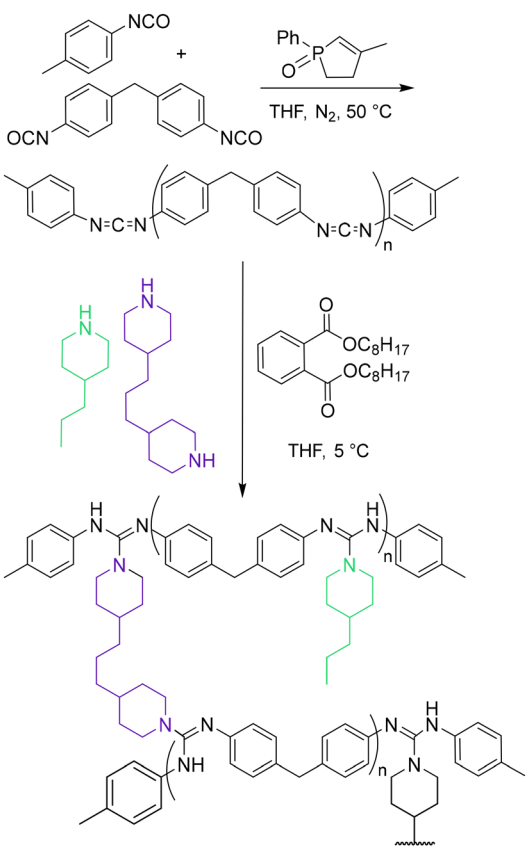

Scheme 1 Synthesis of multifunctional carbodiimide oligomer and preparation of guanidine-based covalent adaptable networks.

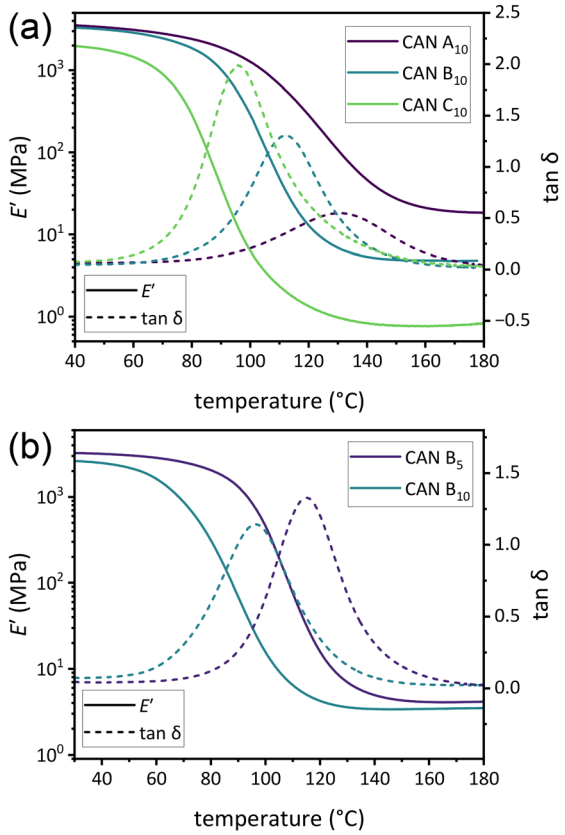

Fig. 2 (a) DMA thermograms of *E*′ *versus* temperature for CAN A_{10}, CAN B_{10}, and CAN C_{10}. (b) DMA thermograms of *E*′ and tan δ *versus* temperature for CAN B_5 and CAN B_{10}.

indicated modest stability as the average temperature at 5% mass loss was found to be 196 °C by TGA (Fig. S10–S16†).

To determine differences in T_g and ν_e, DMA temperature ramps were performed on all CANs (Fig. S17–S30†). T_g was found to vary directly with ν_e, with a larger decrease between CANs A and B than between CANs B and C (Fig. 2a and Table 1). Increased plasticizer was also found to decrease T_g. For example, T_g of CAN A_0 was approximately 44 °C higher than that of CAN A_5 (176 and 132 °C, respectively). This high T_g precluded further rheological analysis of samples without plasticizer, as the temperature window between T_g and the onset of thermal degradation was very limited. Additionally, trends in ν_e of plasticized samples (estimated as $3E'/RT$)[45] in the rubbery plateau at 175 °C were observed to correspond with relative loadings of difunctional : monofunctional amine during synthesis, with little difference between CANs with 5% w/w and 10% w/w plasticizer loadings (Fig. 2b and Table 1).

Table 1 Thermorheological data of CANs from DMA and SAOS rheometry

CAN	T_g (°C)	ν_e (mmol g^{-1})	τ^*_{SR} (s)	τ^*_{cross} (s)	τ^*_{SR} @ T_g +35 °C (s)
A_5	132 ± 1.3[a]	4.49 ± 0.41[a]	129 ± 32[a]	126 ± 22[a]	405 ± 55[a]
A_{10}	126 ± 5.5[b]	4.52 ± 0.46[b]	122 ± 9[b]	159 ± 7[a]	>1200[c]
B_5	113 ± 2.8[a]	1.23 ± 0.07[a]	73 ± 11[a]	98 ± 6[a]	621 ± 16[a]
B_{10}	104 ± 8.0[b]	1.11 ± 0.18[b]	56 ± 9[b]	69 ± 21[b]	>1200[c]
C_5	110 ± 4.0[b]	0.260 ± 0.06[b]	23 ± 9[a]	33 ± 2[a]	327 ± 32[a]
C_{10}	104 ± 7.5[b]	0.296 ± 0.08[b]	38 ± 9[b]	43 ± 14[b]	>1200[c]
A_0	176	—[d]	—[d]	—[d]	—[d]

[a] Data from three samples. [b] Data from two samples. [c] No peak maximum observed in continuous relaxation spectra during experimental window (1200 s). [d] Limited thermal window for analysis precluded determination.

As a means of comparing τ^* of each system, a series of small-amplitude oscillatory shear (SAOS) frequency sweeps were performed at 175 °C using parallel plate shear rheometry within the linear viscoelastic region (Fig. S31–S37†). Relaxation times estimated by the modulus crossover (τ^*_{cross}) possessed a direct relationship to ν_e at both 5% w/w and 10% w/w plasticizer (Fig. 3a and Table 1). The relaxation processes at these temperatures thus appear to be dependent upon crosslinking dynamics, as the amount of reactive species remains constant across all CAN compositions. This is similar to findings in other CANs with equal concentrations of reactive groups, which also possess a direct relationship between ν_e and τ^*.[32,34] Additionally, τ^*_{cross} values were not observed to vary consist-

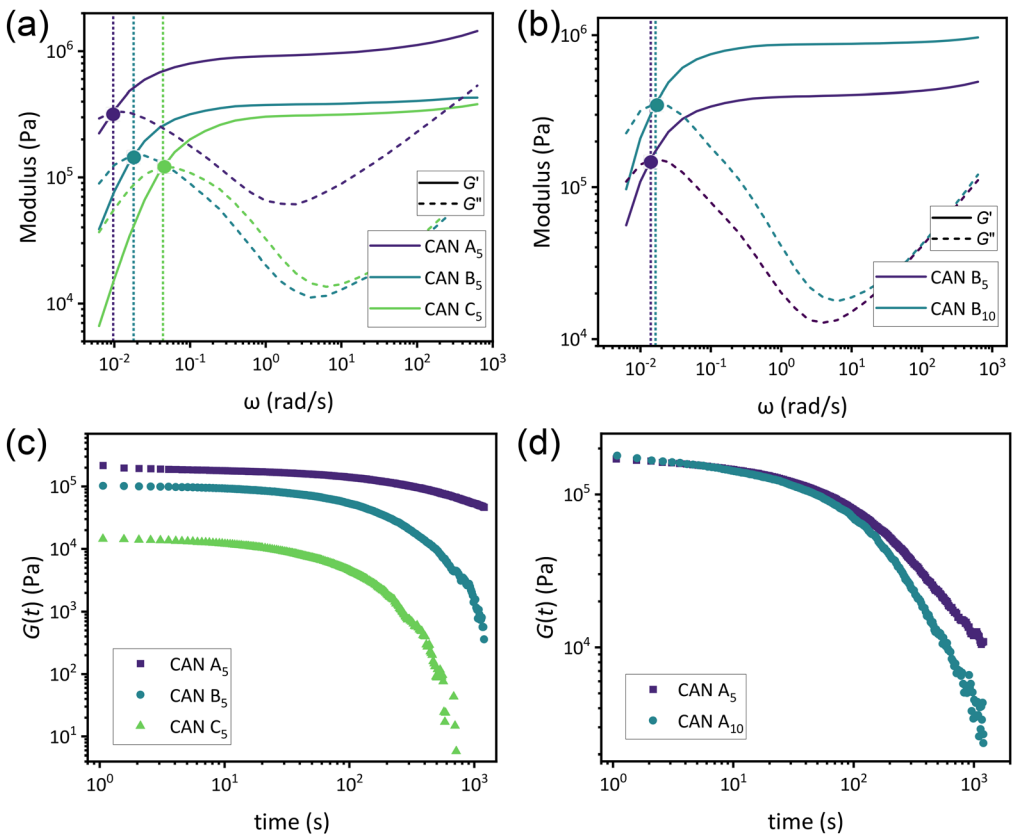

Fig. 3 (a) Frequency sweep data for representative samples of CAN A_5, CAN B_5, and CAN C_5 at 175 °C, where vertical lines indicate crossover frequencies. (b) Frequency sweep data for data for representative samples of CAN B_5 and CAN B_{10} at 175 °C, where vertical lines indicate crossover frequencies. (c) Stress relaxation data for representative samples of CAN A_5, CAN B_5, and CAN C_5 at 175 °C. (d) Stress relaxation data for representative samples of CAN A_5 and CAN A_{10} at 175 °C.

ently as a function of changing plasticizer loading between CAN_5 and CAN_{10} (Fig. 3b and Table 1). As a complementary method of analysis, τ^* at 175 °C was also estimated from stress relaxation experiments (τ^*_{SR}). Some samples exhibited relaxation processes that were not well-captured by fitting the data to a stretched exponential function. As an alternative, we estimated τ^*_{SR} from the principal peak in the continuous relaxation spectra derived from stress relaxation data (Fig. S38–S43†).[46–48] These spectra more clearly distinguished the principal relaxation mode from others such as segmental Rouse relaxation, which was observable at short timescales in some compositions. Trends remained similar to those found in frequency sweeps: a direct relationship to ν_e and no consistent difference due to plasticizer loading was observed (Fig. 3c and d). Additionally, τ^* values were generally in relatively good agreement across the two analysis techniques (Table 1). Previous studies have implicated differences in T_g as important governors of CAN relaxation behavior.[26,49,50] To examine this possibility, we also compared τ^*_{SR} values 35 °C above T_g of each individual network. These values did not exhibit trends similar to those observed at an absolute temperature (Table 1). Thus, temperature relative to T_g does not appear to have predictive value with respect to relaxation behavior, and plasticizer can serve to decouple T_g from CAN dynamics.

Flow activation energies were determined by conducting both frequency sweep and stress relaxation experiments in 5 °C increments above T_g and subsequently constructing master curves by time–temperature superposition (TTS) using both horizontal and vertical shift factors (a_T and b_T, respectively). While rigorous use of TTS relies on the assumption of thermorheological simplicity, CANs cannot possess this characteristic as they exhibit inherently different temperature dependencies of relaxation processes.[46] Nevertheless, previous researchers have found judicious application of TTS to be a valuable means of understanding CAN behavior,[10,51,52] and collapse of data in reduced van Gurp–Palmen plots (Fig. 4a and S44a–49a†) supported the validity of TTS in our systems.[53] While all CAN B and CAN C variants exhibited superposition of both frequency sweep and stress relaxation data from 145–180 °C, TTS only applied from 165–185 °C in CAN A (Fig. 4b, c and S44b–e to S49b–e†). Across all formulations, a_T exhibited an Arrhenius relationship with temperature (Fig. 4d and S44f–S49f†), with similar shifts occurring among SAOS and stress relaxation data. Thus, E_a was calculated using a_T compiled from all experiments on each individual CAN formulation (Table 2),[10] and little variation was observed based on either ν_e or plasticizer loading. This contrasts with associative systems, which tend to exhibit changes in E_a with varying ν_e even with the same concentration of reactive functionalities.[33,34] The interpretation of

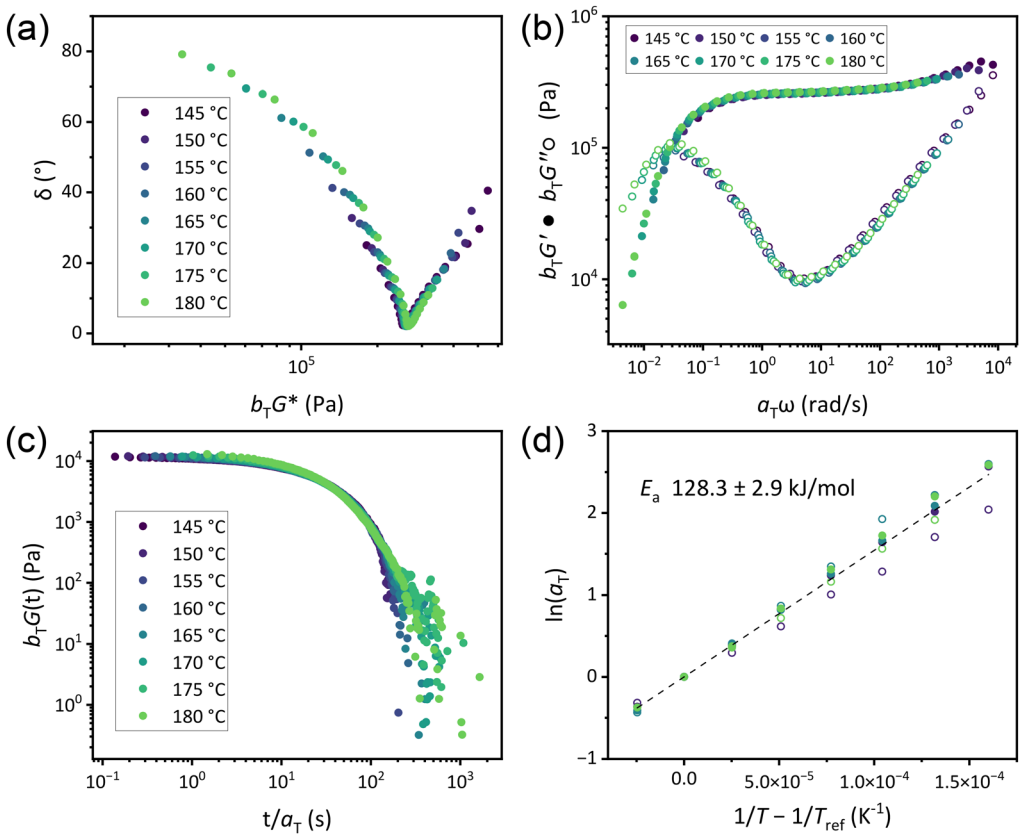

Fig. 4 (a) Reduced van Gurp–Palmen plot of a representative sample of CAN C_5. (b) Master curve of frequency sweep data constructed *via* TTS of a sample of CAN C_5. (c) Master curve of stress relaxation constructed from TTS of a sample of CAN C_5. (d) Arrhenius analysis of horizontal shift factors for all CAN C_5 samples. Filled circles are from frequency sweep data and empty circles from stress relaxation; each color is a single sample. Dashed line is line of best fit. T_{ref} = 175 °C for all analyses.

Table 2 Flow activation energy (kJ mol^{-1}) by Arrhenius analysis of combined shift factors from frequency sweep and stress relaxation data

	5% w/w plasticizer	10% w/w plasticizer
CAN A	136.1 ± 2.8[b,c]	138.5 ± 5.2[a,c]
CAN B	134.7 ± 3.2[b]	146.3 ± 4.0[a]
CAN C	128.3 ± 2.9[b]	134.5 ± 2.6[a]

[a] Combined linear fit from two samples. [b] Combined linear fit from three samples. [c] Data from 165–185 °C; all other data from 145–180 °C.

b_T in this system is less clear (Fig. S50†). In stress relaxation experiments, G_0 and the attendant b_T varied as expected for a dissociative system in which ν_e decreases with increasing temperature. However, b_T from SAOS frequency sweeps exhibited more variation. Previous studies of dissociative CANs have found Arrhenius relationships of b_T with temperature in both types of measurement corresponding to the enthalpy of the dissociation reaction.[10] Such findings were predicted to occur in a limited temperature range and are dependent on the thermodynamics of each specific system. Additionally, b_T in associative CANs is highly variable.[51,52] As any potential side reaction resulting in permanent crosslinking would occur in both experiments and no significant changes were observed in the IR spectra of CANs after rheological analysis (Fig. S51†), a possible explanation for the lack of observed trends in b_T derived from frequency sweeps is a complex interplay between the crosslink dissociation equilibrium, changes in material density, and entropic contributions to elasticity which manifest more substantially on the timescale of the SAOS plateau modulus.

Our findings that τ^* varies directly with ν_e while E_a does not can be rationalized based on the sticky Rouse model developed for unentangled CANs.[52,54] A key component of this model is that the longest relaxation times are directly related to both the crosslink lifetime (τ_{xl}) and the number of crosslinks per chain, *i.e.* ν_e, in accordance with our results (see ESI† for additional discussion).[55] In CANs, τ_{xl} is determined by contributions of (1) the kinetics of the crosslink exchange reaction; (2) Rouse dynamics, which describe chain diffusion based on repeat unit friction; and (3) the mobility of exchanging functionalities within the polymer matrix. As contributions from (1) and (2) are largely determined by the chemical makeup of the system, their temperature dependence is not expected to vary across different ν_e. However, the relatively constant E_a we observe implies that the mobility of exchanging functionalities is not substantially impacted by ν_e in dissociative guanidine-based CANs, similar to another dissociative system with constant functional group concentration[32] and contrasting with vitrimers.[33,34] We hypothesize this difference originates in the temperature dependence on ν_e that is not present in associative systems.

Conclusions

In conclusion, we have analyzed the effects of ν_e and plasticizer on rheological properties of guanidine-based CANs using complementary rheometric techniques. The combination of multifunctional carbodiimide oligomers with specific ratios of difunctional to monofunctional secondary alkyl amine species enabled the synthesis of CANs with varying ν_e but a constant concentration of reactive groups. By changing ν_e in three levels and plasticizer loading by weight in three levels, a library of seven CANs was developed. T_g was found to vary directly with ν_e and plasticizer loading. However, τ^* obtained by both stress relaxation and SAOS frequency sweeps varied directly with ν_e while plasticizer had little effect; thus, plasticizer serves to decouple τ^* from T_g. Further, we observed a relatively constant E_a across all network compositions, in contrast with studies of associative CANs. We hope our studies motivate additional investigation of the fundamental properties of vitrimer-like dissociative systems, further illustrate the utility of TTS in rheological analysis of CANs, and add plasticizer content to the growing list of characteristics that can be used to tune CAN dynamics.

Data availability

The data supporting this article have been included in the main text and as part of the ESI.

Conflicts of interest

There are no conflicts to declare.

Acknowledgements

We acknowledge the National Science Foundation (DMR 2105149) and the Karen and Joseph Morse Summer Research Fellowship for support of this work. The authors thank Dr Ralm Ricarte for helpful discussions of rheological characterization and analysis, Dr Mark Peyron for guidance on statistical analysis, and Kyle Mikkelsen for assistance with characterization techniques.

References

1 C. J. Kloxin, T. F. Scott, B. J. Adzima and C. N. Bowman, Covalent Adaptable Networks (CANs): A Unique Paradigm in Cross-Linked Polymers, *Macromolecules*, 2010, **43**(6), 2643–2653, DOI: 10.1021/ma902596s.
2 R. J. Wojtecki, M. A. Meador and S. J. Rowan, Using the Dynamic Bond to Access Macroscopically Responsive Structurally Dynamic Polymers, *Nat. Mater.*, 2011, **10**(1), 14–27, DOI: 10.1038/nmat2891.
3 C. N. Bowman and C. J. Kloxin, Covalent Adaptable Networks: Reversible Bond Structures Incorporated in Polymer Networks, *Angew. Chem., Int. Ed.*, 2012, **51**(18), 4272–4274, DOI: 10.1002/anie.201200708.

4 M. K. McBride, B. T. Worrell, T. Brown, L. M. Cox, N. Sowan, C. Wang, M. Podgorski, A. M. Martinez and C. N. Bowman, Enabling Applications of Covalent Adaptable Networks, *Annu. Rev. Chem. Biomol. Eng.*, 2019, **10**(1), 175–198, DOI: **10.1146/annurev-chembioeng-060718-030217**.

5 X. Chen, M. A. Dam, K. Ono, A. Mal, H. Shen, S. R. Nutt, K. Sheran and F. Wudl, A Thermally Re-Mendable Cross-Linked Polymeric Material, *Science*, 2002, **295**(5560), 1698–1702, DOI: **10.1126/science.1065879**.

6 B. T. Michal, C. A. Jaye, E. J. Spencer and S. J. Rowan, Inherently Photohealable and Thermal Shape-Memory Polydisulfide Networks, *ACS Macro Lett.*, 2013, **2**(8), 694–699, DOI: **10.1021/mz400318m**.

7 D. Montarnal, M. Capelot, F. Tournilhac and L. Leibler, Silica-Like Malleable Materials from Permanent Organic Networks, *Science*, 2011, **334**(6058), 965–968, DOI: **10.1126/science.1212648**.

8 W. Denissen, J. M. Winne and F. E. D. Prez, Vitrimers: Permanent Organic Networks with Glass-like Fluidity, *Chem. Sci.*, 2015, **7**(1), 30–38, DOI: **10.1039/C5SC02223A**.

9 M. Podgórski, B. D. Fairbanks, B. E. Kirkpatrick, M. McBride, A. Martinez, A. Dobson, N. J. Bongiardina and C. N. Bowman, Toward Stimuli-Responsive Dynamic Thermosets through Continuous Development and Improvements in Covalent Adaptable Networks (CANs), *Adv. Mater.*, 2020, **32**(20), 1906876, DOI: **10.1002/adma.201906876**.

10 A. Jourdain, R. Asbai, O. Anaya, M. M. Chehimi, E. Drockenmuller and D. Montarnal, Rheological Properties of Covalent Adaptable Networks with 1,2,3-Triazolium Cross-Links: The Missing Link between Vitrimers and Dissociative Networks, *Macromolecules*, 2020, **53**(6), 1884–1900, DOI: **10.1021/acs.macromol.9b02204**.

11 P. Chakma, C. N. Morley, J. L. Sparks and D. Konkolewicz, Exploring How Vitrimer-like Properties Can Be Achieved from Dissociative Exchange in Anilinium Salts, *Macromolecules*, 2020, **53**(4), 1233–1244, DOI: **10.1021/acs.macromol.0c00120**.

12 W.-X. Liu, C. Zhang, H. Zhang, N. Zhao, Z.-X. Yu and J. Xu, Oxime-Based and Catalyst-Free Dynamic Covalent Polyurethanes, *J. Am. Chem. Soc.*, 2017, **139**(25), 8678–8684, DOI: **10.1021/jacs.7b03967**.

13 G. M. Scheutz, J. J. Lessard, M. B. Sims and B. S. Sumerlin, Adaptable Crosslinks in Polymeric Materials: Resolving the Intersection of Thermoplastics and Thermosets, *J. Am. Chem. Soc.*, 2019, **141**(41), 16181–16196, DOI: **10.1021/jacs.9b07922**.

14 B. J. Adzima, H. A. Aguirre, C. J. Kloxin, T. F. Scott and C. N. Bowman, Rheological and Chemical Analysis of Reverse Gelation in a Covalently Cross-Linked Diels–Alder Polymer Network, *Macromolecules*, 2008, **41**(23), 9112–9117, DOI: **10.1021/ma801863d**.

15 M. Bin Rusayyis and J. M. Torkelson, Recyclable Polymethacrylate Networks Containing Dynamic Dialkylamino Disulfide Linkages and Exhibiting Full Property Recovery, *Macromolecules*, 2020, **53**(19), 8367–8373, DOI: **10.1021/acs.macromol.0c01539**.

16 L. Li, X. Chen and J. M. Torkelson, Covalent Adaptive Networks for Enhanced Adhesion: Exploiting Disulfide Dynamic Chemistry and Annealing during Application, *ACS Appl. Polym. Mater.*, 2020, **2**(11), 4658–4665, DOI: **10.1021/acsapm.0c00720**.

17 R. Martin, A. Rekondo, A. R. de Luzuriaga, G. Cabañero, H. J. Grande and I. Odriozola, The Processability of a Poly (Urea-Urethane) Elastomer Reversibly Crosslinked with Aromatic Disulfide Bridges, *J. Mater. Chem. A*, 2014, **2**(16), 5710–5715, DOI: **10.1039/C3TA14927G**.

18 B. Zhang, Z. A. Digby, J. A. Flum, P. Chakma, J. M. Saul, J. L. Sparks and D. Konkolewicz, Dynamic Thiol–Michael Chemistry for Thermoresponsive Rehealable and Malleable Networks, *Macromolecules*, 2016, **49**(18), 6871–6878, DOI: **10.1021/acs.macromol.6b01061**.

19 H. Ying, Y. Zhang and J. Cheng, Dynamic Urea Bond for the Design of Reversible and Self-Healing Polymers, *Nat. Commun.*, 2014, **5**(1), 3218, DOI: **10.1038/ncomms4218**.

20 Y. Zhang, H. Ying, K. R. Hart, Y. Wu, A. J. Hsu, A. M. Coppola, T. A. Kim, K. Yang, N. R. Sottos, S. R. White and J. Cheng, Malleable and Recyclable Poly(Urea-Urethane) Thermosets Bearing Hindered Urea Bonds, *Adv. Mater.*, 2016, **28**(35), 7646–7651, DOI: **10.1002/adma.201601242**.

21 L. Zhang and S. J. Rowan, Effect of Sterics and Degree of Cross-Linking on the Mechanical Properties of Dynamic Poly(Alkylurea–Urethane) Networks, *Macromolecules*, 2017, **50**(13), 5051–5060, DOI: **10.1021/acs.macromol.7b01016**.

22 J. J. Lessard, K. A. Stewart and B. S. Sumerlin, Controlling Dynamics of Associative Networks through Primary Chain Length, *Macromolecules*, 2022, **55**(22), 10052–10061, DOI: **10.1021/acs.macromol.2c01909**.

23 Y. Liu, Z. Tang, J. Chen, J. Xiong, D. Wang, S. Wang, S. Wu and B. Guo, Tuning the Mechanical and Dynamic Properties of Imine Bond Crosslinked Elastomeric Vitrimers by Manipulating the Crosslinking Degree, *Polym. Chem.*, 2020, **11**(7), 1348–1355, DOI: **10.1039/C9PY01826C**.

24 T. Isogai and M. Hayashi, Critical Effects of Branch Numbers at the Cross-Link Point on the Relaxation Behaviors of Transesterification Vitrimers, *Macromolecules*, 2022, **55**(15), 6661–6670, DOI: **10.1021/acs.macromol.2c00560**.

25 P. Miao, X. Leng, J. Liu, G. Song, M. He and Y. Li, Regulating the Dynamic Behaviors of Transcarbamoylation-Based Vitrimers via Mono-Variation in Density of Exchangeable Hydroxyl, *Macromolecules*, 2022, **55**(12), 4956–4966, DOI: **10.1021/acs.macromol.2c00127**.

26 Y. Spiesschaert, C. Taplan, L. Stricker, M. Guerre, J. M. Winne and F. E. D. Prez, Influence of the Polymer Matrix on the Viscoelastic Behaviour of Vitrimers, *Polym. Chem.*, 2020, **11**(33), 5377–5385, DOI: **10.1039/D0PY00114G**.

27 B. Soman and C. M. Evans, Effect of Precise Linker Length, Bond Density, and Broad Temperature Window on the

Rheological Properties of Ethylene Vitrimers, *Soft Matter*, 2021, **17**(13), 3569–3577, DOI: **10.1039/D0SM01544J**.

28 S. K. Schoustra, T. Groeneveld and M. M. J. Smulders, The Effect of Polarity on the Molecular Exchange Dynamics in Imine-Based Covalent Adaptable Networks, *Polym. Chem.*, 2021, **12**(11), 1635–1642, DOI: **10.1039/D0PY01555E**.

29 Y. Feng, H. Qiu, P. Deng, Z. Nie, J. Chen, K. Gong, X. Fan and S. Qi, Tuning the Static and Dynamic Properties of Epoxy Vitrimers through Modulation of Cross-Link Density, *Eur. Polym. J.*, 2023, **196**, 112308, DOI: **10.1016/j.eurpolymj.2023.112308**.

30 L. Yang, L. Li, L. Fu, B. Lin, Y. Wang and C. Xu, Design of Ester Crosslinked Rubber with High Dynamic Properties by Increasing Dynamic Covalent Bond Density, *Polym. Chem.*, 2022, **13**(48), 6650–6661, DOI: **10.1039/D2PY01165D**.

31 M. M. Obadia, A. Jourdain, P. Cassagnau, D. Montarnal and E. Drockenmuller, Tuning the Viscosity Profile of Ionic Vitrimers Incorporating 1,2,3-Triazolium Cross-Links, *Adv. Funct. Mater.*, 2017, **27**(45), 1703258, DOI: **10.1002/adfm.201703258**.

32 D. J. Fortman, J. P. Brutman, M. A. Hillmyer and W. R. Dichtel, Structural Effects on the Reprocessability and Stress Relaxation of Crosslinked Polyhydroxyurethanes, *J. Appl. Polym. Sci.*, 2017, **134**(45), 44984, DOI: **10.1002/app.44984**.

33 M. Hayashi and R. Yano, Fair Investigation of Cross-Link Density Effects on the Bond-Exchange Properties for Trans-Esterification-Based Vitrimers with Identical Concentrations of Reactive Groups, *Macromolecules*, 2020, **53**(1), 182–189, DOI: **10.1021/acs.macromol.9b01896**.

34 R. Hajj, A. Duval, S. Dhers and L. Avérous, Network Design to Control Polyimine Vitrimer Properties: Physical Versus Chemical Approach, *Macromolecules*, 2020, **53**(10), 3796–3805, DOI: **10.1021/acs.macromol.0c00453**.

35 L. Chen, L. Zhang, P. J. Griffin and S. J. Rowan, Impact of Dynamic Bond Concentration on the Viscoelastic and Mechanical Properties of Dynamic Poly(Alkylurea-Co-Urethane) Networks, *Macromol. Chem. Phys.*, 2020, **221**(1), 1900440, DOI: **10.1002/macp.201900440**.

36 L. Li, X. Chen, K. Jin and J. M. Torkelson, Vitrimers Designed Both To Strongly Suppress Creep and To Recover Original Cross-Link Density after Reprocessing: Quantitative Theory and Experiments, *Macromolecules*, 2018, **51**(15), 5537–5546, DOI: **10.1021/acs.macromol.8b00922**.

37 M.-J. Xie, C.-C. Wang, R. Zhang, J. Cao, M.-Z. Tang and Y.-X. Xu, Length Effect of Crosslinkers on the Mechanical Properties and Dimensional Stability of Vitrimer Elastomers with Inhomogeneous Networks, *Polymer*, 2024, **290**, 126550, DOI: **10.1016/j.polymer.2023.126550**.

38 O. Konuray, S. Moradi, A. Roig, X. Fernández-Francos and X. Ramis, Thiol–Ene Networks with Tunable Dynamicity for Covalent Adaptation, *ACS Appl. Polym. Mater.*, 2023, **5**(3), 1651–1656, DOI: **10.1021/acsapm.2c02136**.

39 A. Safaei, S. Terryn, B. Vanderborght, G. Van Assche and J. Brancart, Toughening and Stiffening in Thermoreversible Diels–Alder Polymer Network Blends, *Macromolecules*, 2023, **56**(11), 4325–4335, DOI: **10.1021/acs.macromol.2c02558**.

40 H. E. Houck, K. A. McConnell, C. J. Klingler, A. L. Koenig, G. K. Himka and M. B. Larsen, Postpolymerization Modification by Nucleophilic Addition to Styrenic Carbodiimides, *ACS Macro Lett.*, 2023, **12**(8), 1112–1117, DOI: **10.1021/acsmacrolett.3c00382**.

41 J. Chen, L. Li, J. Luo, L. Meng, X. Zhao, S. Song, Z. Demchuk, P. Li, Y. He, A. P. Sokolov and P.-F. Cao, Covalent adaptable polymer networks with CO_2-facilitated recyclability, *Nat. Commun.*, 2024, **15**, 6605, DOI: **10.1038/s41467-024-50738-7**.

42 A. P. Gies, W. H. Heath, R. J. Keaton, J. J. Jimenez and J. J. Zupancic, MALDI-TOF/TOF CID Study of Polycarbodiimide Branching Reactions, *Macromolecules*, 2013, **46**, 7616–7637, DOI: **10.1021/ma401481g**.

43 A. J. Melchor Bañales and M. B. Larsen, Thermal Guanidine Metathesis for Covalent Adaptable Networks, *ACS Macro Lett.*, 2020, **9**(7), 937–943, DOI: **10.1021/acsmacrolett.0c00352**.

44 V. Ramirez, E. B. V. Pelt, R. K. Pooni, A. J. M. Bañales and M. B. Larsen, Thermodynamic, Kinetic, and Mechanistic Studies of the Thermal Guanidine Metathesis Reaction, *Org. Biomol. Chem.*, 2022, **20**(29), 5861–5868, DOI: **10.1039/D_2OB01036D**.

45 P. C. Hiemenz and T. Lodge, *Polymer Chemistry*, CRC Press, Boca Raton, 2nd edn, 2007, pp. 446.

46 R. G. Ricarte and S. Shanbhag, A Tutorial Review of Linear Rheology for Polymer Chemists: Basics and Best Practices for Covalent Adaptable Networks, *Polym. Chem.*, 2024, **15**(9), 815–846, DOI: **10.1039/D3PY01367G**.

47 S. C. Grindy, R. Learsch, D. Mozhdehi, J. Cheng, D. G. Barrett, Z. Guan, P. B. Messersmith and N. Holten-Andersen, Control of hierarchical polymer mechanics with bioinspired metal-coordination dynamics, *Nat. Mater.*, 2015, **14**, 1210–1216, DOI: **10.1038/nmat4401**.

48 J. S. A. Ishibashi, I. C. Pierce, A. B. Chang, A. Zografos, B. M. El-Zaatari, Y. Fang, S. J. Weigand, F. S. Bates and J. A. Kalow, Mechanical and Structural Consequences of Associative Dynamic Cross-Linking in Acrylic Diblock Copolymers, *Macromolecules*, 2021, **54**, 3972–3986.

49 S. Wang, S. Ma, Q. Li, W. Yuan, B. Wang and J. Zhu, Fire-Safe, Monomer-Recovery, Highly Malleable Thermosets from Renewable Resources, *Macromolecules*, 2018, **51**, 8001–8012.

50 G. Lee, H. Y. Song, S. Choi, C. B. Kim, K. Hyun and S. Ahn, Harnessing β-Hydroxyl Groups in Poly(β-Amino Esters) toward Robust and Fast Reprocessing Covalent Adaptable Networks, *Macromolecules*, 2022, **55**, 10366–10376.

51 M. L. Martins, X. Zhao, Z. Demchuk, J. Luo, G. P. Carden, G. Toleutay and A. P. Sokolov, Viscoelasticity of Polymers with Dynamic Covalent Bonds: Concepts and Misconceptions, *Macromolecules*, 2023, **56**, 8688–8696, DOI: **10.1021/acs.macromol.3c01545**.

52 R. G. Ricarte, S. Shanbhag, D. Ezzeddine, D. Barzycki and K. Fay, Time-Temperature Superposition of Polybutadiene Vitrimers, *Macromolecules*, 2023, **56**, 6806–6817, DOI: 10.1021/acs.macromol.3c00883.
53 H. Y. Song, G. Lee, S. Ahn and K. Hyun, Linear Viscoelasticity of Covalent Adaptable Network (CAN) Polymers Comprising β-Amino Esters, *Korea-Aust. Rheol. J.*, 2023, **35**(2), 69–79, DOI: 10.1007/s13367-023-00054-1.
54 R. G. Ricarte and S. Shanbhag, Unentangled Vitrimer Melts: Interplay between Chain Relaxation and Cross-link Exchange Controls Linear Rheology, *Macromolecules*, 2021, **54**, 3304–3320, DOI: 10.1021/acs.macromol.0c02530.
55 R. H. Colby, X. Zheng, M. H. Rafailovich, J. Sokolov, D. G. Peiffer, S. A. Schwarz, Y. Strzhemechny and D. Nguyen, Dynamics of Lightly Sulfonated Polystyrene Ionomers, *Phys. Rev. Lett.*, 1998, **81**, 3786–3789, DOI: 10.1103/PhysRevLett.81.3876.